Limnol. Oceanogr., 51(2), 2006, 973–987

Natural growth rates in Antarctic krill (*Euphausia superba*): II. Predictive models based on food, temperature, body length, sex, and maturity stage

Angus Atkinson,[1] *Rachael S. Shreeve, Andrew G. Hirst*
British Antarctic Survey, Natural Environment Research Council, High Cross, Madingley Rd, Cambridge CB3 OET, United Kingdom

Peter Rothery
Natural Environment Research Council, Centre for Ecology and Hydrology, CEH Monks Wood, Abbots Ripton, Huntingdon PE28 2LS, United Kingdom

Geraint A. Tarling, David W. Pond, Rebecca E. Korb, Eugene J. Murphy, and Jonathon L. Watkins
British Antarctic Survey, Natural Environment Research Council, High Cross, Madingley Road, Cambridge CB3 OET, United Kingdom

Abstract

We used the instantaneous growth rate method to determine the effects of food, temperature, krill length, sex, and maturity stage on in situ summer growth of krill across the southwest Atlantic sector of the Southern Ocean. The main aims were to examine the separate effects of each variable and to generate a predictive model of growth based on satellite-derivable environmental data. Both growth increments in length on moulting (GIs) and daily growth rates (DGRs, mm d^{-1}) ranged greatly among the 59 swarms, from 0.58–15% and 0.013–0.32 mm d^{-1}. However, all swarms maintained positive mean growth, even those in the low chlorophyll *a* (Chl *a*) zone of the central Scotia Sea. Among a suite of indices of food quantity and quality, large-scale monthly Chl *a* values from SeaWiFS predicted krill growth the best. Across our study area, the great contrast between bloom and nonbloom regions was a major factor driving variation in growth rates, obscuring more subtle effects of food quality. GIs and DGRs decreased with increasing krill length and decreased above a temperature optimum of 0.5°C. This probably reflects the onset of thermal stress at the northern limit of krill's range. Thus, growth rates were fastest in the ice edge blooms of the southern Scotia Sea and not at South Georgia as previously suggested. This reflects both the smaller size of the krill and the colder water in the south being optimum for growth. Males tended to have higher GIs than females but longer intermoult periods, leading to similar DGRs between sexes. DGRs of equivalent-size krill tended to decrease with maturity stage, suggesting the progressive allocation of energy toward reproduction rather than somatic growth. Our maximum DGRs are higher than most literature values, equating to a 5.7% increase in mass per day. This value fits within a realistic energy budget, suggesting a maximum carbon ration of ~20% d^{-1}. Over the whole Scotia Sea/South Georgia area, the gross turnover of krill biomass was ~1% d^{-1}.

High-latitude ecosystems provide case studies of how environmental variability and change affect marine organisms. These ecosystems are characterized by low seasonal variation in temperatures, yet they are the fastest warming regions on the planet (Vaughan et al. 2003). They also exhibit great variability in phytoplankton abundance, which is related to narrow seasonal windows of primary production. Consequently, polar invertebrates tend to be stenothermal, sensitive even to slight changes in temperature, with life cycles timed with phytoplankton blooms (Clarke 1988). Thus, polar ectotherms might be particularly sensitive to environmental change (Peck et al. 2004).

Antarctic krill, *Euphausia superba*, exemplify the potential sensitivity of polar species to change. This key species is stenothermal, and completion of its life cycle depends on blooms at critical times of the year (Quetin et al. 1994; Quetin and Ross 2001). Over 50% of krill stocks are located in the southwest Atlantic sector (Atkinson et al. 2004), a region of rapid upper ocean warming (Meredith and King 2005), loss of winter sea ice (Parkinson 2002), and great interannual variability in chlorophyll *a* (Chl *a*) concentrations (Constable et al. 2003).

Experimental approaches have revealed how environmental variability affects krill physiology (Ikeda 1985; Quetin et al. 1994). However, krill are an active, swarming species that do not feed, respire, or grow at natural rates under long-term captivity (Quetin et al. 1994). One component of the energy budget is, nevertheless, measurable without such problems. Growth in euphausiids can be measured with the instantaneous growth rate (IGR) method, in a way as free as possible from laboratory artefacts (Quetin et al. 1994; Nicol 2000;

[1] Corresponding author (aat@bas.ac.uk).

Acknowledgments

We thank the captain, officers, and crew of the RRS *James Clark Ross* for their professional support during sampling, Peter Ward for running the 2002 cruise, Doug Bone for maintaining the nets, and Kate Arnold for her enthusiastic help with netting. Steve Nicol generously shared a design for the mass-rearing tanks for growth experiments and discussed methodology. Andrew Fleming accessed the SeaWiFS data, provided courtesy of NASA. Comments from two reviewers greatly improved the analysis and presentation of this article. This is a contribution to the DYNAMOE Programme of the British Antarctic Survey.

Tarling et al. 2006). The IGR approach does not expose the workings of the energy budget but measuring growth reveals the overall net benefit to the animal; in other words, it provides one overall index of suitability of the environment. Thus, the ability to predict growth directly from food and temperature helps to gauge the likely effects of future change in each of these parameters.

Uncertainties over the growth rate of krill constrain studies of their population dynamics and overall secondary production, as well as their energy budget (Quetin et al. 1994; Murphy and Reid 2001; Fach et al. 2002). Obtaining time series of length frequencies from the wild has been the most common approach (Mackintosh 1972; Rosenberg et al. 1986), but it requires repeated sampling of a single population, without bias from advection (Fach et al. 2002), sampler selectivity (Reid et al. 2002), or mortality (Pakhomov 2000). By contrast, the IGR method measures growth directly and over shorter timescales (Quetin et al. 1994; Nicol 2000). Despite these advantages, only five studies have used this method on postlarvae, and only Ross et al. (2000) related growth to environmental variability. Data on natural growth rates of krill are sparse and conflicting. Two length frequency-based studies suggest maxima of >0.3 mm d^{-1} (Clarke and Morris 1983; Reid 2001), nearly three times that of any published value from the IGR method.

We used the IGR method during two summers to examine how food, temperature, body length, sex, and maturity stage combine to dictate growth rates. By measuring a spectrum of krill sizes across the range of conditions in the southwest Atlantic sector, these effects can be teased apart to develop predictive models of growth. Part I (Tarling et al. 2006) refines the IGR method and develops a model to predict intermoult period. Here in Part II, we examine first the factors that influence the length increase per moult. Then we combine intermoult periods and length increments to derive daily growth rates (mm d^{-1}) and develop models to predict these. We also calculate mass-specific growth to place our results in the context of an energy budget and to estimate the gross rate of increase in krill biomass across the southwest Atlantic sector.

Methods

The cruises and sampling stations are illustrated in Tarling et al. (2006), which should also be referred to for the details of the IGR methodology. Here we provide a summary overview of the 59 IGR experiments (Table 1), explain their design, describe the environmental variables, and formulate the growth model.

Principle of the IGR method—Although growth in mass is a near-continuous process, crustaceans grow in length in a series of steps, coinciding with each moult. We define the growth increment, GI, as the percentage change in length on moulting and the period between moults as the intermoult period, IMP (days). The IGR method, where krill are maintained individually for a few days to observe moulting, allows the measurement of both GI and IMP. GI is obtainable from the increase in length between the old exoskeleton and the freshly moulted animal, based on measurements of the uropods. IMP is the inverse of the daily moulting frequency. The basic principle of the IGR method is that the measured GI captures all of the growth of krill length during its IMP. The daily average rate of length increase is the descriptor of growth used in population dynamics. For each of the 1,749 animals that moulted during our incubations, we can calculate a theoretical equivalent daily growth rate, DGR (mm d^{-1}), as a function of GI and IMP. DGR is calculated using Eq. 2 in Tarling et al. (2006):

$$DGR = \frac{L_{pre} \times GI}{IMP \times 100} \quad (1)$$

where GI is calculated using Eq. 4 in Tarling et al. (2006) and L_{pre} is the length of each krill before moulting. This cannot be measured and is calculated from Eq. 10 in Tarling et al. (2006):

$$L_{pre} = \frac{(L \times 100)}{(100 + GI)} \quad (2)$$

where L is the measured length of the animal shortly after moulting.

Because GI and IMP are separate components of growth, we have examined the controlling factors separately. Thus, the companion Part I (Tarling et al. 2006) investigates the controls on IMP, while here we examine the controls on GI and ultimately on DGR. Our end result is the development of predictive functional relationships between DGR and food, temperature, krill length, and maturity stage.

Improvements in IGR methodology—The analysis in this article benefits from improvements in IGR methodology (Tarling et al. 2006). The problem with GI measured in the traditional way was that, with each successive day of our ~5-d incubation period, the GIs of moulting krill tended to decline. This is not unprecedented (fig. 1 in Nicol et al. 1992), and we found that the decline was most pronounced in swarms with the fastest growth. So probably the inability to feed during the incubations progressively reduces the GIs of the moulters. Based on the rates of these declines, we have corrected our measured GIs to in situ values, defined as those at the start of the experiment.

Our IMP values are also calculated by an improved method. The standard method is based on the number of krill moulting in relation to the number incubated in each experiment. This leads to an average IMP estimate for a group of krill, preventing the IMPs of the component individuals (ranging in size and thus in IMP) to be elucidated. Swarms may also moult synchronously, further biasing estimates. Therefore, we have calculated the IMP of each individual krill from a model of all the krill incubated (Tarling et al. 2006). This model allowed prediction of IMP from the variables found to affect it, namely krill length, maturity stage, and temperature.

Experimental design—The surveys were conducted aboard RRS *James Clark Ross* in January–February of 2002 (South Georgia) and 2003 (Scotia Sea and South Georgia), with stations for krill sampling summarized in Table 1 and illustrated in Fig. 1 of Tarling et al. (2006). Krill were caught

Table 1. Mean values of krill growth for each site, with a summary of ancillary data. An asterisk indicates that two adjacent krill swarms were sampled and experimented on separately (at the other sites, only one swarm was sampled). GIs include the actual mean values measured over the 5-d incubation period and corrected in situ values (Tarling et al. 2006). Food indices include the nearest shipboard surface value to the krill fishing, with values in parentheses showing maximum water column Chl *a* value for Scotia Sea stations (where deep Chl *a* maxima were encountered).

					GI (% per IMP)					Food concentration (mg Chl *a* m^{-3})		
Site	Date (day, month, year)	No. of krill incubated (number of molters)	Mean krill length (mm)	Most abundant maturity stage	Measured (standard method)	Corrected (Tarling et al. 2006)	DGR (mm d^{-1})	Growth in mass, G (%d^{-1})	Env. temp. (°C)	Surface value (max in water column)	SeaWiFS mean value within 100 km	SeaWiFS max value within 100 km
1	6 Jan 02	14 (3)	42	MS1	2.58	4.22	0.092	0.844	3.0	6.5	1.7	8.1
2	7 Jan 02	54 (14)	40	FS	5.00	6.65	0.157	1.602	3.1	2.9	2.2	8.1
3*	7 Jan 02	413 (100)	40	FS	6.67	8.57	0.184	2.162	3.0	2.9	2.2	8.1
4*	11 Jan 02	395 (110)	41	FS	7.29	10.15	0.221	2.373	3.7	2.6	3.9	16
5	13 Jan 02	56 (6)	53	MS2	4.34	5.44	0.125	1.017	3.7	10	3.2	12
6	16 Jan 02	120 (22)	39	FS	3.22	4.1	0.0932	0.942	3.6	10	4.7	19
7*	16 Jan 02	314 (55)	40	FS	2.38	3.24	0.0726	0.722	3.8	10	4.8	19
8*	18 Jan 02	123 (44)	40	FS	1.88	2.96	0.0670	0.654	3.8	0.22	0.66	3.4
9	18 Jan 02	163 (49)	39	FS	1.45	2.65	0.0602	0.603	3.3	0.22	0.66	3.4
10*	19 Jan 02	119 (43)	40	FS	1.59	2.69	0.0612	0.618	3.3	0.97	0.68	3.1
11	23 Jan 02	384 (113)	46	FS	2.88	4.44	0.0959	0.891	3.7	2.7	0.71	3.4
12*	23 Jan 02	108 (30)	43	FS	3.06	5.09	0.115	1.076	3.6	1.2	3.3	17
13	26 Jan 02	232 (90)	42	FS	3.31	5.25	0.118	1.134	3.9	6.3	4.0	17
14	26 Jan 02	69 (30)	46	MS2	1.61	2.64	0.0600	0.529	3.9	3.3	3.3	18
15*	28 Jan 02	86 (27)	43	FS	1.75	2.97	0.0676	0.598	4.4	1.2	2.0	14
16	30 Jan 02	87 (12)	54	FA5	2.05	2.65	0.0408	0.311	4.8	1.9	4.5	17
17*	31 Jan 02	274 (25)	41	MS2	1.29	2.29	0.0513	0.487	4.1	2.5	2.7	16
18*	4 Feb 02	288 (4)	41	MS1	3.69	4.41	0.101	0.968	4.7	2.1	2.0	14
19	10 Jan 03	300 (45)	34	MS1	0.84	1.19	0.0242	0.311	2.0	0.072 (0.24)	0.24	0.63
20	11 Jan 03	240 (45)	31	MS1	1.90	3.3	0.0712	0.936	0.85	0.096 (0.23)	0.27	2.1
21	12 Jan 03	150 (27)	33	FS/MS1	2.09	3.33	0.0738	1.119	−0.14	0.17 (0.30)	0.23	1.6
22	12 Jan 03	168 (39)	30	J	3.70	5.47	0.118	1.840	0.49	0.15 (0.31)	0.3	2.3
23	14 Jan 03	90 (6)	50	FA3	2.09	3.45	0.0974	0.842	3.0	0.57 (0.98)	0.33	0.75
24	16 Jan 03	300 (70)	42	FA3	2.42	3.84	0.102	1.127	2.1	0.66 (0.82)	0.64	19
25	17 Jan 03	298 (45)	40	MS2	3.08	4.7	0.12	1.344	1.3	0.92 (0.93)	0.47	1.2
26	18 Jan 03	229 (88)	30	J	10.4	13.7	0.305	5.650	0.089	1.1 (1.2)	1.5	9.7
27	19 Jan 03	90 (24)	44	FA3	0.66	1.41	0.0392	0.382	−0.85	0.57 (1.1)	0.54	14
28*	22 Jan 03	210 (25)	41	FA3	0.56	1.14	0.0254	0.301	2.2	0.55 (0.61)	0.25	0.53
29*	23 Jan 03	384 (94)	40	J	2.02	3.06	0.0761	0.875	1.27	0.98 (1.0)	0.27	0.57
30*	26 Jan 03	258 (89)	32	J	1.05	1.94	0.0480	0.679	−0.057	0.2 (0.41)	0.2	0.26
31	26 Jan 03	90 (24)	38	FS	1.54	2.5	0.0594	0.716	−0.20	0.13 (0.27)	0.16	0.27
32	27 Jan 03	138 (10)	48	FA3	0.54	1.05	0.0273	0.246	2.7	0.20 (0.44)	0.21	0.39
33	28 Jan 03	150 (31)	42	FS	2.69	3.78	0.0830	0.904	2.9	0.14 (0.77)	0.15	0.31
34*	1 Feb 03	306 (41)	49	FA5	0.21	0.58	0.0142	0.181	2.8	0.090 (0.29)	0.38	6.8
35*	2 Feb 03	300 (45)	51	FA5	0.15	0.48	0.0134	0.119	2.2	0.065 (0.21)	0.18	0.43
36	4 Feb 03	186 (59)	36	J	10.8	15.2	0.318	5.062	0.87	0.84 (0.79)	0.79	2.7
37*	7 Feb 03	298 (34)	50	FA5	1.9	2.92	0.0701	0.682	2.26	0.6 (0.86)	0.97	2.6
38*	8 Feb 03	282 (27)	54	FA5	0.32	0.76	0.0174	0.128	3.28	0.18 (0.48)	0.92	6.4
39	13 Feb 03	390 (51)	47	J	2.88	4.36	0.0993	0.962	4.1	12	2.5	16
40	15 Feb 03	156 (24)	47	J	2.84	4.18	0.101	0.947	4.3	5.4	2.5	10
41*	15 Feb 03	222 (47)	47	J	3.18	4.8	0.117	1.149	4.3	6.7	2.4	8.7
42	17 Feb 03	24 (1)	42	J	5.45	5.85	0.143	1.540	—	1.0	1.2	5

with a Rectangular Midwater Trawl (RMT 8) fitted with two nets that were opened and closed remotely to sample 59 swarms of krill. The environmental variability was wide: 0.07–10 mg Chl *a* m^{-3}, −0.85°C to 4.8°C, and the krill ranged from 24 to 61 mm in length (juveniles to mature, postspawning females). This variability allowed us to tease apart the effect of each variable on GI and DGR, as described below.

Predictive models of krill growth—We used nonlinear models to predict krill growth simultaneously from food, temperature, krill length, sex, and maturity stage. We stress that growth varies seasonally as well, but time of year is not included in our models because the sampling was in midsummer, confined to a narrow seasonal window characterised by prebloom and bloom conditions.

We used quadratic functions to represent length, based on a general dome-shaped relationship between DGR and length (Fig. 1), which is supported by independent models of growth (Ikeda 1985; Siegel 1987). For the food term, we used a three-parameter hyperbola model:

$$Growth = a + \frac{(d \times Food)}{(e + Food)} \quad (3)$$

where *a*, *d*, and *e* are constants. This relationship has Michaelis–Menten parameters and is thus of the type used previously for krill (Ross et al. 2000). However, it does not force the function through the origin because growth can be negative during starvation, i.e., when food concentrations become very low (Quetin et al. 1994). Quadratic functions of temperature were chosen, based on prior analyses (not reported here), which found maximal growth at intermediate temperatures, having allowed for the effects of length and food. The complete nonlinear model to predict GI and DGR was thus constructed as:

$$Growth = a + b \times Length + c \times Length^2 + [d \times Food/(e + Food)] + f \times Temperature + g \times Temperature^2 + H \quad (4)$$

where *a*, *b*, *c*, *d*, *e*, *f*, and *g* are constants and the units of *Length*, *Food*, and *Temperature* are, respectively, mm (from front of eye to tip of telson), mg Chl *a* m^{-3}, and °C. *H* is a random effect for unexplained variation. The krill were divided into four groups according to sex and maturity stage, following Tarling et al. (2006). These were juveniles, males, immature females, and mature females. Most (93%) of male moulters were immature, so this group is comparable in maturity stage with immature females. Models were fitted both considering and ignoring these sex and maturity differences.

Models were fitted by ordinary least squares using Genstat 6. This analysis produces standard errors for the model parameters based on the assumption that the observations on individual krill are statistically independent. This is unlikely because krill from the same swarm (with the same environmental variables) are more likely to be similar than those from different swarms, i.e., an effect of pseudo-replication. To allow for this, we estimated components of between- and within-swarm variation and calculated robust standard errors using the method of Diggle et al. (1994).

Testing goodness of fit of the models—The goodness of fit of the models was tested using partial residuals. This allows examination of the fit of the model separately for length, food, and temperature, having adjusted each measured growth value for the effects of the other variables in turn, i.e., food and temperature, length and temperature, and length and food, respectively. Thus, for example, the partial residual for length, r_L is calculated as:

$$r_L = DGR - d(Food)/(e + Food) - f(Temperature) - g(Temperature^2) \quad (5)$$

Thus, when the model fits the data, a plot of the r_L values against length should follow the fitted line for a quadratic relationship with *Length* in Eq. 4. For presentation, partial residuals have been scaled so that their means match those of the observed growth rates.

Mass-specific growth rates—Natural rates of growth in krill mass are not measurable directly, and it is necessary to make assumptions to estimate this parameter. We have used the approach of Shreeve et al. (2005), in which length–mass regressions are applied to measured increases in length.

To measure length–mass relationships, krill were frozen (−80°C) immediately on capture from each of the sites sampled in 2002. In the United Kingdom, 30 krill from each site were thawed and sex and maturity stage were determined according to Tarling et al. (2006). Length was measured from front of the eye to the tip of the telson, and krill were then freeze dried for 24 h under a vacuum and weighed (±10 μg) on a Mettler AT 250 balance.

In the first instance, length–mass regressions were constructed separately for each site to test for any change within the sampling period, such as a gradual fattening of krill in preparation for winter (Results: morphometric relationships). No such trends were found, so data from all stations were pooled. However, it remained necessary to make sex- and maturity stage-specific regressions because of differences in the body compositions of krill (Schmidt et al. 2004).

Daily mass specific growth rates, *G*, were estimated as:

$$G = 100\left(\frac{M - M_{pre}}{M_{pre} \times IMP}\right) \quad (6)$$

where *M* is the mass after moulting and M_{pre} is the mass at the beginning of the preceding *IMP*. These were calculated from the respective krill lengths, *L* and L_{pre}, using our sex- and maturity stage-specific length–mass regressions. The factor 100 converts the values to percentages to make them comparable with daily carbon rations (see Discussion: energy budget of krill).

Environmental variables—Supporting environmental data are available from SeaWiFS, underway sampling, and water sampling at conductivity-temperature-depth (CTD) stations near the krill capture sites (Table 2). Below, we describe how these data were collected and used as predictors of krill growth.

Temperature: Two measurements of temperature were taken. These were the mean inlet temperature of the pumped

Table 2. Summary of coverage of the various types of food indices during the two cruises.

Food proxy	Source of data	Total number of measurement points
SeaWiFS Chl *a*	SeaWiFS monthly composites	313 pixels per station*
Shipboard surface Chl *a*	CTD profiles plus 6.5-m nontoxic supply	891 samples
Maximum Chl *a* in water column	CTD profiles only	130 profiles
Integrated (0–100 m) Chl *a*	CTD profiles only	130 profiles
POC values	CTD water at 20 m depth	126 samples
Polyunsaturated and total fatty acids	CTD water at 20 m depth	107 samples
Counts of microplankton taxa	CTD water at 20 m depth	139 samples

* Mean number of 9 × 9 km pixels of data available for averaging per station.

nontoxic seawater supply during the capture of each krill swarm and, second, the mean of the daily measurements within the krill incubation tanks. These two were highly correlated, although incubation temperatures were in a narrower range, with higher minimum and lower maximum values compared with environmental temperatures.

SeaWIFS-derived Chl *a*: Monthly SeaWiFS level-3 standard mapped image (SMI) products of Chl *a* concentration were plotted in relation to our sampling sites. Using Arc GIS 8.2, we selected every 9 × 9 km Chl *a* pixel value within a 100-km radius of each krill sampling site, and calculated the mean and maximum and upper quartile pixel value from this output file. We extracted data for the monthly SeaWiFS composites according to the date on which each station was sampled. If the sampling date was after the middle of the month, just that month's composite was used, but if it was before the middle of the month, we extracted the relevant pixels from that month's composite plus those from the month before and analyzed the combined output.

Shipboard-derived Chl *a*: During both cruises, water sample profiles from the CTD casts were augmented with hourly samples taken from the ship's nontoxic supply, taken ~6.5 m below the sea surface. Chl *a* concentrations were analyzed with standard fluorometric techniques (Parsons et al. 1984), described for the 2003 cruise in Korb et al. (in press). The 2002 cruise differed only in that Chl *a* was extracted from the filters immediately aboard ship rather than freezing before analysis. Integrated values of Chl *a* (mg Chl *a* m^{-2} within the top 100-m layer) were obtained at each CTD station with a calibrated fluorometer mounted on the CTD.

We used these measurements to produce three food datasets. These comprised (1) ''surface'' Chl *a*, a merged dataset comprising the hourly values from the nontoxic supply and those from the CTD stations at the equivalent 6.5 m depth; (2) maximum Chl *a*, the maximum value from each CTD cast (deep Chl *a* maxima were observed); and (3) integrated Chl *a*, the integrated (0–100 m) values within the water column.

POC, fatty acids, and microplankton taxa: At the CTD stations in the vicinity of each krill net haul, additional food indices were obtained from water samples collected at 20 m depth. Fatty acids and particulate organic carbon (POC) were measured with standard methodology (*see* Ward et al. 2005). Microplankton taxa were counted with the Utermöhl (1958) technique, from 50-mL water samples fixed in 1% acid Lugol's solution. Only the cells >~10 μm were enumerated, with 16 taxonomic categories identified (Table 3). We used an inverted microscope and carried out two or three perpendicular transects across the whole diameter of the chamber receptacle at ×100 magnification. From these measurements, we extracted indices that capture aspects of food quality as well as quantity. These comprise POC, the polyunsaturated fatty acids 20 : 5(n-3), 22 : 6(n-3), total fatty acids, total large diatoms, total small diatoms, total ciliates plus dinoflagellates, and total counted cells of all taxa.

Matching time and space scales of food indices to those of krill sampling—In order to predict krill growth, we tested a variety of food indices and methods of integrating their spatial coverage. The shipboard-derived food indices were derived first from the nearest water sample to the krill swarm. Second, for those indices with better spatial coverage (SeaWiFS and Shipboard surface Chl *a*), we also used values integrated over the area within 100 km of the swarm. These wider scales are required for SeaWiFS, whose coverage was restricted by cloud and ice cover.

Results

Overall range of growth rates—Table 1 summarizes all growth rates and environmental conditions across the two study seasons. DGRs in our study encompass the wide range of values obtained previously for krill (Fig. 1), with the two highest values approximating the maxima recorded. Figure 1 also fits broadly to the bell-shaped relationship between DGR and length predicted by Ikeda (1985).

Spatial variation in growth rates and population structure—Growth rates ranged greatly during both cruises (Table 1), this being illustrated in Fig. 2a for the second, wider scale, cruise. However, stations with high growth showed only weak congruence to regions of plentiful food. This reflects the interplay among krill length, temperature, and food. Across the whole Scotia Sea, there was a general gradient in population structure, from large krill in the northeast toward smaller krill in the southwest, with some bimodal distributions in between (Fig. 2b). Together with the 5°C temperature variation across this range, this conspired to obscure clear effects from food.

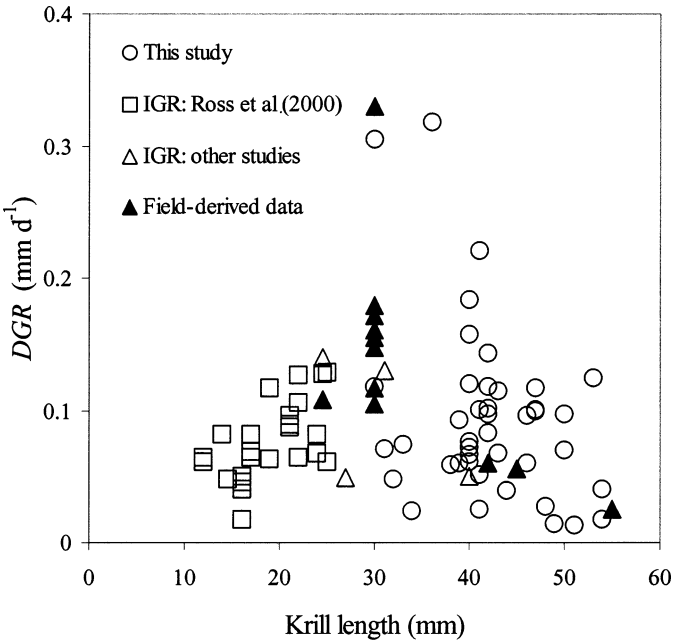

Fig. 1. *Euphausia superba.* Comparison of average DGR values from each site (Table 1) with available spring/summer literature data from IGR measurements (Morris and Keck 1984; Buchholz 1985; Daly 1998; Ross et al. 2000) and net-derived length frequency data (Kanda et al. 1982; Clarke and Morris 1983; Rosenberg et al. 1986; McClatchie 1988).

Variation in growth within and between swarms—Among the individual krill sampled at a site, there was great variability in measured GI values. This scatter reflects only partly differences in krill length and maturity stage; there was also a high degree of unexplainable, between-animal variability in GI (see Results: predictive model of GI and DGR). However, in contrast with the variability within swarms and between stations, the mean GIs of adjacent swarms sampled at a station were very similar (Fig. 3). Of the 17 neighboring pairs of swarms sampled, only 3 had GIs differing by >1% per IMP between the pair.

Comparison of food indices to predict growth—We compared our suite of food indices in the model (Eq. 4) to investigate which was the best predictor of growth. Large-scale monthly food indices from SeaWiFS were by far the best at predicting growth (Table 4), based on the R^2 values of the fitted model. The other food indices either had lower R^2 values or returned unrealistic parameter values during the fitting process. All models below therefore incorporated mean SeaWiFS-derived Chl *a* within 100 km of the krill sampling, as this is also most amenable to extraction from satellite images for input to large-scale models of krill growth.

There was a general positive relationship between the various food indices (e.g., Fig. 4). This is despite the fact that these integrate over a very wide range of scales, from just a single 50-mL Lugol's sample taken near the krill swarm to the vast area within a 100-km radius of it. The consistent relationship between krill growth and these various food indices reflects the correlation between food indices across these scales.

Table 3. Microplankton taxa enumerated in cell counts on Lugol's-preserved samples.

Broader grouping for analysis	Microplankton taxon
Ciliates and dinoflagellates	Ciliates >10 μm
	Dinoflagellates >10 μm
Small diatoms	*Thalassiosira* spp.
	Nitzschia/Pseudonitzschia spp.
	Chaetoceros spp.
	Fragilariopsis kerguelensis
	Thalassionema/Fragilariopsis spp.
Large diatoms	*Odontella* spp.
	Eucampia antarctica
	Corethron spp.
	Rhizosolenia/Proboscia spp.
	Thalassiothrix spp.
	Unidentified species 1
	Unidentified species 2

Predictive models of GI and DGR—A series of models were fitted (Table 5) to predict both GI and DGR. Two formulations of these are presented. The first and simplest is for all krill combined, i.e., ignoring the effects of sex and maturity stage (models 1, 3, and 5). This allows predictions where the investigator is not able, or does not need, to differentiate according to maturity stage. The more refined analysis (models 2 and 4) fits the model with common terms for length, food, and temperature but with variable intercepts to allow for the different growth rates between sexes and maturity stages. There is evidence for significant effects of sex and maturity-stage categories on DGR ($F_{3,1739} = 24.88$, $p < 0.05$) and on GI ($F_{3,1739} = 27.79$, $p < 0.05$). However, models 2 and 4, which incorporate this sex/maturity-stage effect, explain only slightly more of the variability in growth than the corresponding models 1 and 3 which ignore these effects. So in studies where sex and maturity stage are not treatable separately, model 3 can be applied with little loss of explanatory power.

With the exception of model 5, the temperature term in all models is environmental temperature, i.e., measured at 6.5 m from the nontoxic intake during krill sampling. Model 5 instead uses the mean incubation temperature. Overall, it yields a similar result to the corresponding model 3 using the closely related environmental temperature, with a slightly higher temperature of maximum growth and a corresponding decline with increasing temperature. For large-scale predictions of DGR, however, models 3 and 4 are appropriate because the indices used are available from remote sensing or large-scale surveys.

Goodness of fit of models—Plots of partial residuals (Fig. 5) show that the model formulation provides a good fit for the various predictor variables. But despite the good basic fit of the models, half of the variation in krill growth remains

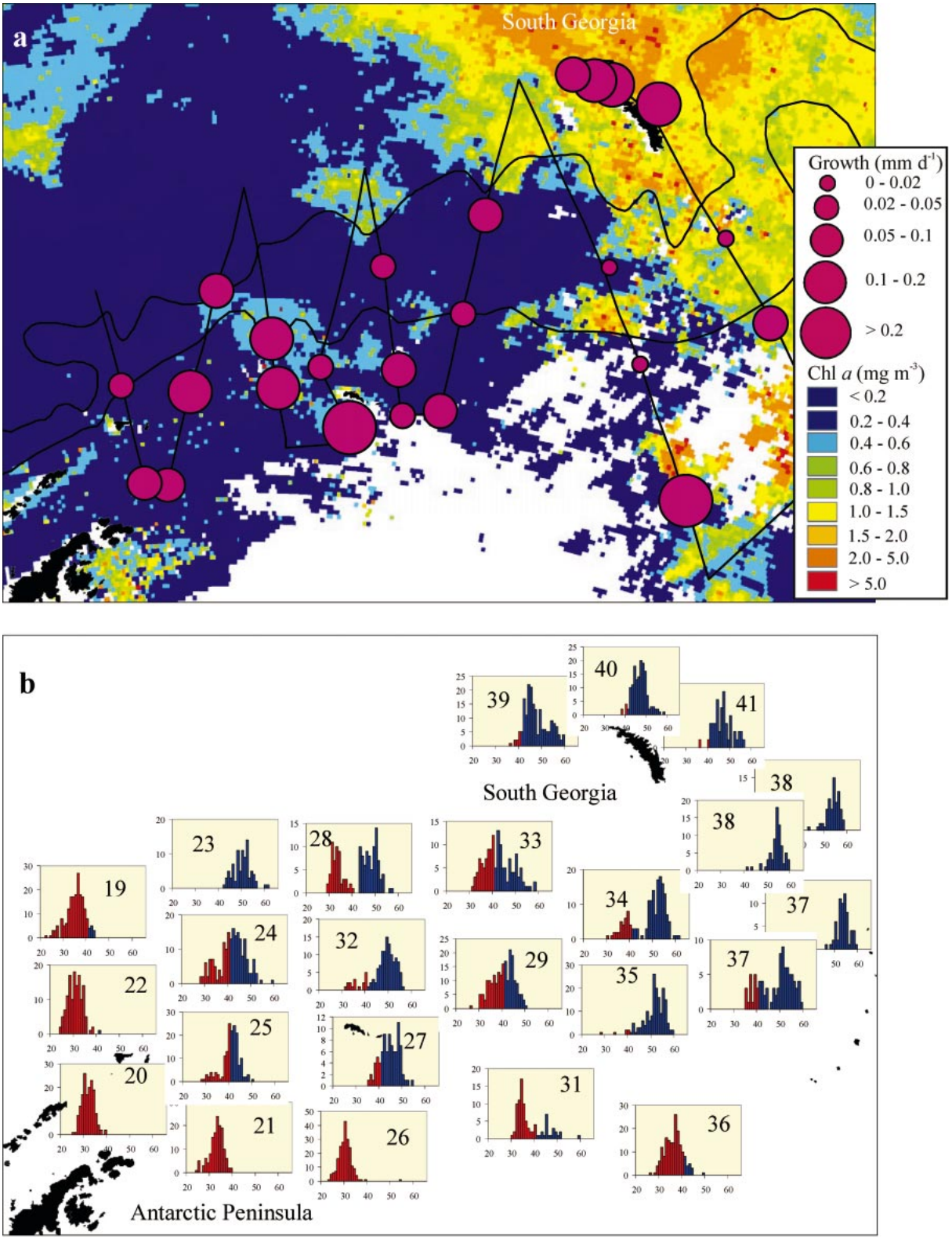

Fig. 2. (a) Mean DGR of krill at the various sampling sites during the 2003 survey, plotted against a composite SeaWiFS image from December 2002 to February 2003. Fronts plotted are the historical positions, from north to south, of the Southern Antarctic Circumpolar Current (ACC) Front (Thorpe et al. 2002) and the Southern Boundary of the ACC (Orsi et al. 1995). (b) Length frequency distributions of krill across the 2003 survey area. A mean of 149 individuals were measured per station, with <40-mm krill in red. Vertical axis gives the actual numbers counted. Histograms are labeled with station numbers and are displaced slightly for clarity; see Tarling et al. (2006) for actual positions.

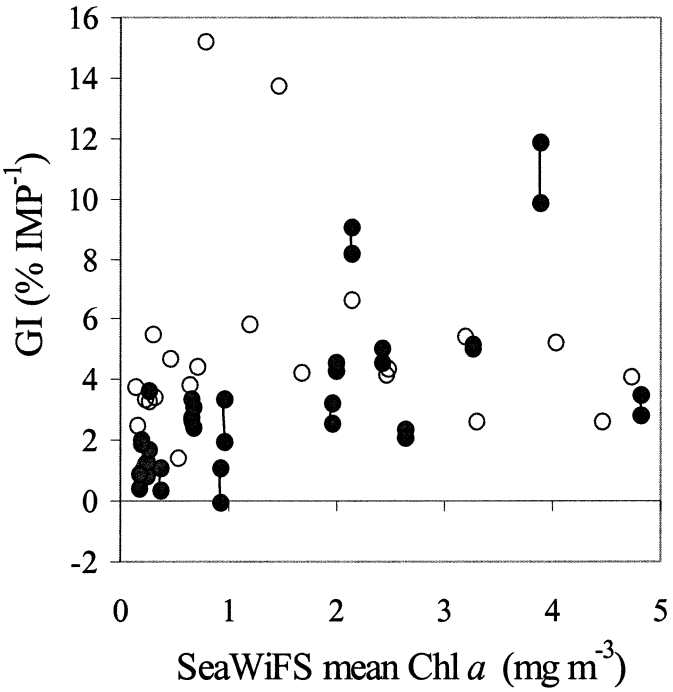

Fig. 3. Mean GI values of all individual swarms. Open symbols are where only one swarm was sampled at a single site, and linked filled symbols represent adjacent swarms sampled at a single site.

unexplained (Table 5). These residuals can be attributed to two sources, namely, between-swarm and within-swarm variability. All krill within a given swarm have the same food and temperature indices in the models, so any variation between equivalent size/maturity-stage krill from a single swarm must reflect natural variability in growth, natural variability in allometric relationships, or measurement imprecision. To partition these residuals we conducted a one-way analysis of variance for models 3 and 4. Of this unexplained variability, 49% (model 3) and 43% (model 4) occurs within swarms. A substantial component is thus unexplainable variation between krill from the same environment. This is not a serious impediment to our model, which is a predictor of mean growth rates of krill, not individual rates. Because krill do not grow continuously in length, DGR values should be modeled as population averages.

Table 4. Comparison of food indices for fitting of model 3 (see Table 5). Listed here are the indices that returned both permissible coefficients and the highest R^2 values. Food proxies are listed in order of R^2 of the fitted model. The R^2 for the mean SeaWiFS Chl *a* is higher than that from the equivalent model in Table 5 because, here, only data from the second cruise was used. This was because of absent data for some food indices on the first cruise, which biases strict comparisons among food indices.

Food proxy	Integration in relation to krill swarm	R^2 (%)
Mean SeaWiFS Chl *a*	Within 100-km radius	64
Upper quartile SeaWiFS Chl *a*	Within 100-km radius	63
Maximum shipboard surface Chl *a*	Within 100-km radius	46
Shipboard surface Chl *a*	Nearest value	46
Mean surface Chl *a*	Within 100-km radius	41
Maximum SeaWiFS Chl *a*	Within 100-km radius	39
Total large diatoms	Nearest value	35
Particulate organic carbon	Nearest value	17

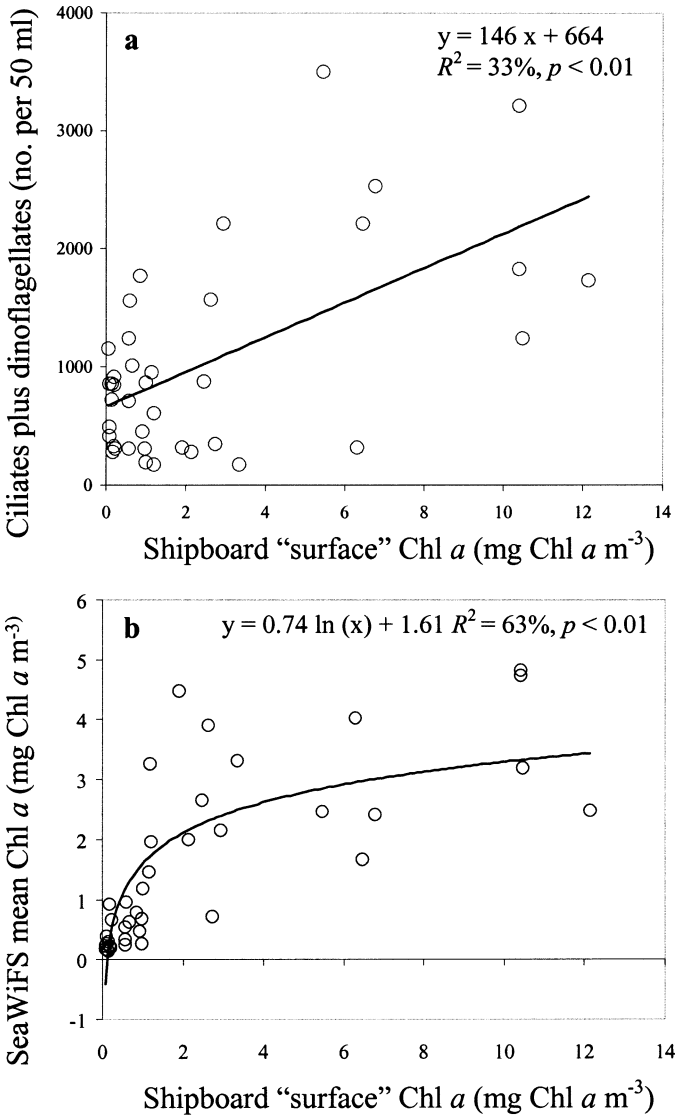

Fig. 4. Relationship among various food indices, derived for each of the 42 krill sampling sites. (a) Ciliates plus dinoflagellates, derived from the Lugol's-preserved sample at 20 m depth nearest to each krill swarm, versus the shipboard Chl *a* value at 6.5 m depth nearest to that swarm. (b) Mean SeaWiFS-derived Chl *a* within 100 km of each krill swarm versus the shipboard of 6.5 m Chl *a* value at a depth nearest to that swarm.

Model predictions—The combined effects of krill length, food, and temperature in model 3 are shown in Fig. 6. The ranges of these predictors encompass the range encountered across the experiments, and the selected lower temperature of 0.5°C is close to that of maximum growth (Table 5; Fig. 5c). Growth is very similar for temperatures <1°C, but declines significantly above this. The quadratic term for length also means that growth rates decline increasingly with

Table 5. Coefficients of models predicting DGR and GI from length, food, and temperature in Eq. 4. Models 1, 3, and 5 are fitted with no differentiation of krill according to sex or maturity stage, whereas models 2 and 4 include an effect for sex and maturity stage, using common coefficients for predictor variables but differing constant terms, *a*. Robust standard errors of coefficients are in parentheses. For predicting daily growth rates, either model 3 (for all krill) or model 4 (sex and maturity-stage specific) should be applied, with units being: krill length in mm from tip of telson to front of eye, food as mean Chl *a* concentration (mg m^{-3}) in vicinity of the krill, and temperature as upper mixed layer values in °C.

Model values		Growth increment, GI		Daily growth rate, DGR		
		Model 1, for all krill	Model 2, maturity-stage specific	Model 3, for all krill	Model 4, maturity-stage specific	Model 5, for all krill, but using incubation temperatures
Constant	(all krill combined), *a*	6.60 (7.89)	—	−0.066 (0.165)	—	0.057 (0.218)
	Juveniles, *a*	—	2.52 (7.46)	—	−0.158 (0.156)	—
	Males, *a*	—	1.13 (7.49)	—	−0.193 (0.156)	—
	Immature females, *a*	—	0.99 (7.53)	—	−0.192 (0.156)	—
	Mature females, *a*	—	−0.40 (7.49)	—	−0.216 (0.156)	—
Length	Linear term, *b*	−0.385 (0.318)	−0.184 (0.293)	0.002 (0.0066)	0.00674 (0.00611)	−0.0019 (0.0076)
	Quadratic term, *c*	0.00259 (0.00369)	0.00107 (0.00342)	−0.000061 (0.000077)	−0.000101 (0.000071)	−0.000036 (0.000087)
Food	Maximum term, *d*	17.53 (4.32)	17.24 (4.16)	0.385 (0.091)	0.377 (0.087)	0.345 (0.113)
	Half saturation constant, *e*	0.332 (0.260)	0.323 (0.246)	0.328 (0.246)	0.321 (0.232)	0.297 (0.287)
Temperature	Linear term, *f*	0.595 (0.841)	0.845 (0.783)	0.0078 (0.017)	0.013 (0.0163)	−0.011 (0.045)
	Quadratic term, *g*	−0.477 (0.217)	−0.548 (0.202)	−0.0101 (0.00045)	−0.0115 (0.00420)	−0.00569 (0.00113)
R^2		48	50	48	50	43
Residual standard deviation, s		3.1	3.1	0.066	0.065	0.069
Temperature of maximum growth, °C		0.6	0.8	0.4	0.5	−0.97

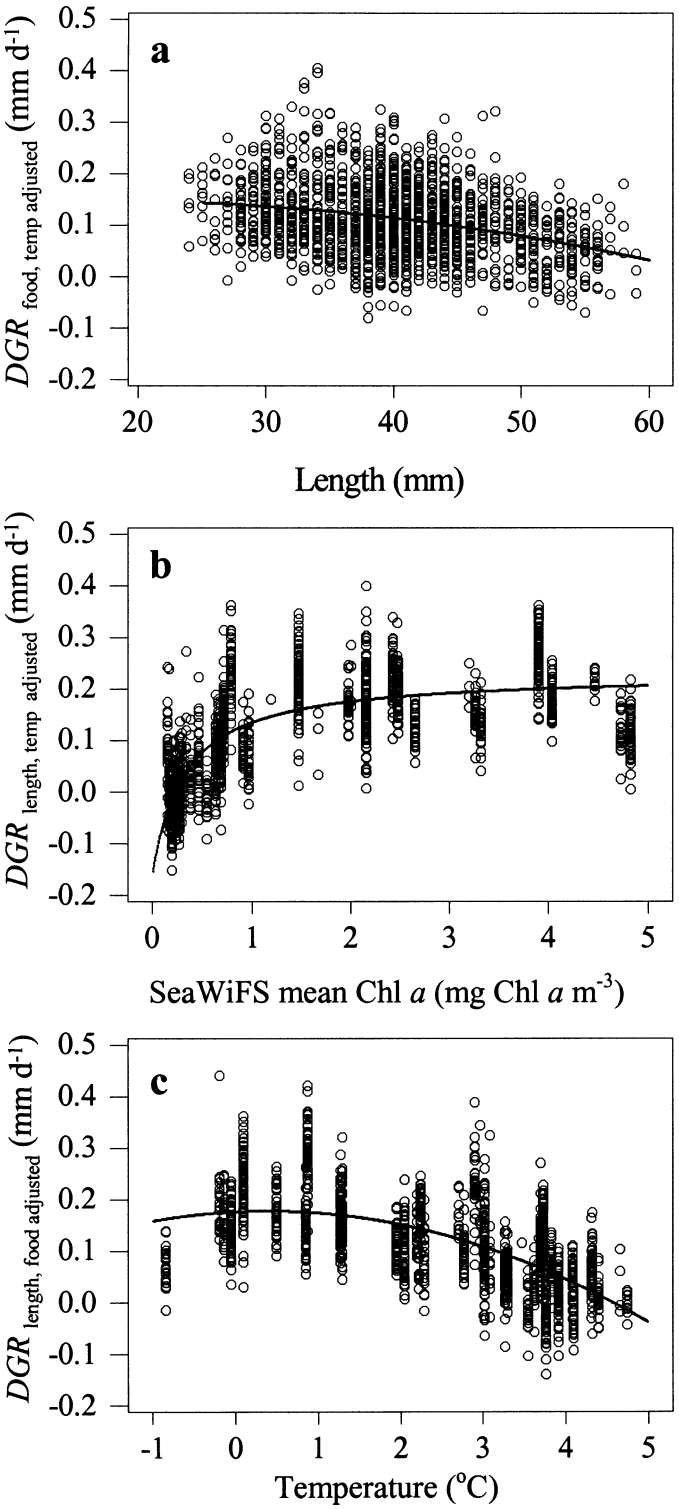

Fig. 5. Partial residuals of DGR plotted against (a) length, (b) food, and (c) environmental temperature, to show the fit of model 3 (line). For explanation, see Methods: testing goodness of fit of the models.

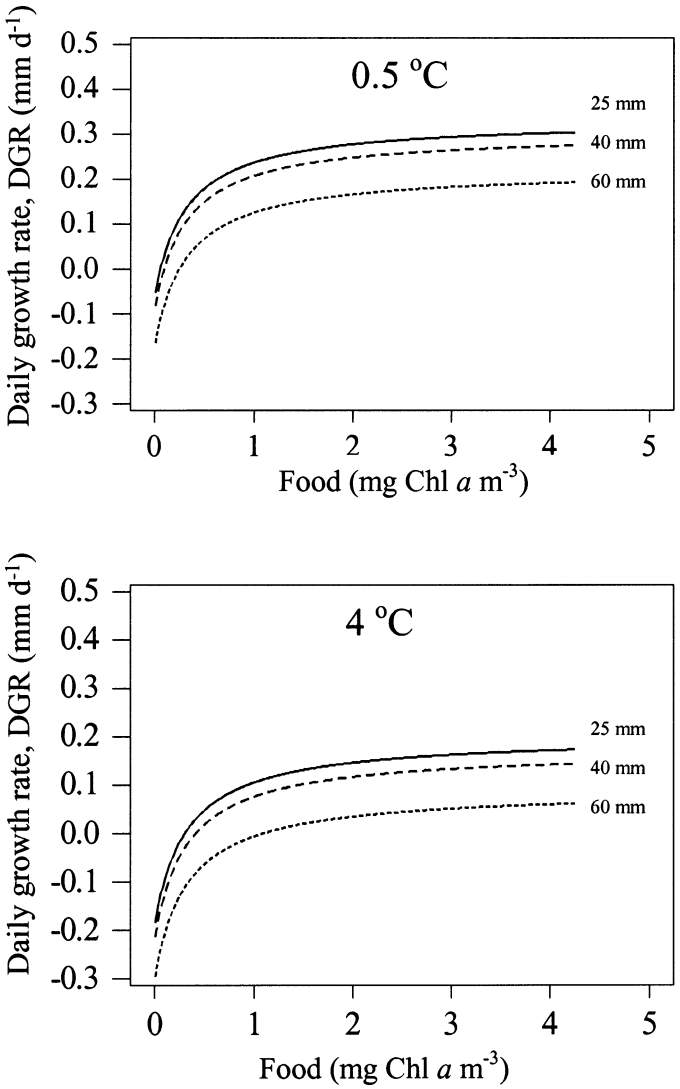

Fig. 6. Predicted DGR based on model 3, over the range of krill lengths, food concentrations, and temperatures in our experiments. The lower temperature of 0.5°C is presented, as it approximates that of maximum DGR.

length. This explains the much greater reduction in DGR between 40 mm and 60 mm compared with that between 25 mm and 40 mm krill.

The effects of maturity stage on DGR (model 4) are reflected in progressively smaller values of the constant *a* (Table 5), so growth declines with increasing maturity stage. However, differences in DGR between sexes of equivalent maturity stage, i.e., between males (mainly immature) and immature females is negligible.

Morphometric relationships—Length–mass regressions were constructed first separately for each site sampled during the first cruise at South Georgia. These allow examination of seasonal effects, as they were all from a relatively localized area north of South Georgia and were done over a 1-month time window. They are expressed in Fig. 7 as the predicted mass of a 40-mm krill, a characteristic size for this

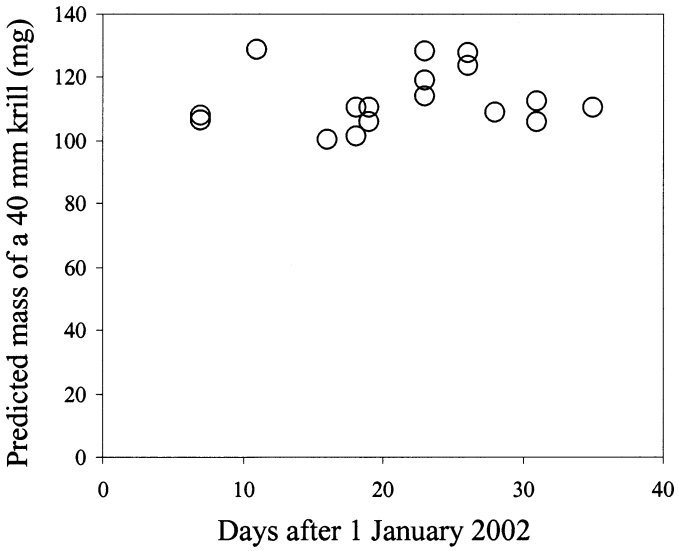

Fig. 7. Predicted mass of a 40-mm krill, based on length–mass regressions from the individual stations on the first cruise. Not plotted here are predictions from one nonsignificant ($p > 0.05$) regression and one regression constructed solely from krill >40 mm in length. Regression analysis showed no significant change in predicted krill mass over time.

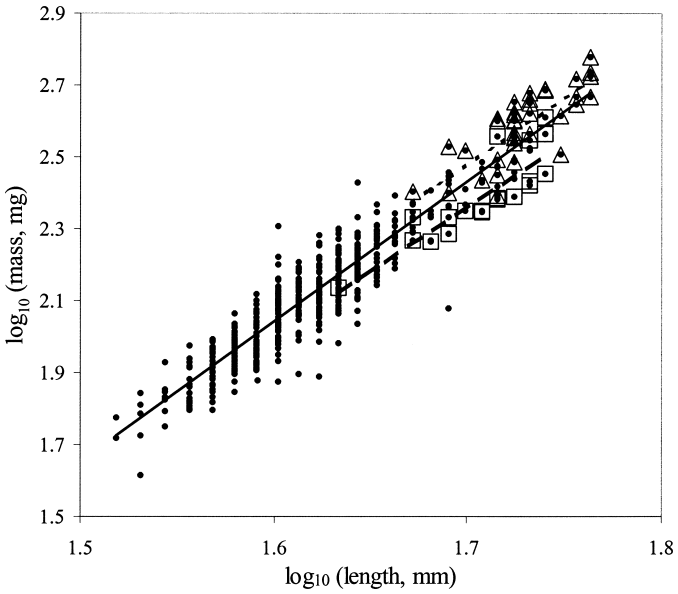

Fig. 8. *Euphausia superba.* Length–dry mass regressions for mature adult males (square symbols, broken line) mature adult females (triangles, dotted line) and for all krill combined (circles, solid line). Regression coefficients are presented in Table 6.

cruise (Table 1). Regression analysis showed no significant shift in morphometrics during the sampling period, as would be associated, for example, with a seasonal fattening of krill. This supports the use of pooled morphometric relationships from which to estimate growth in krill mass.

These pooled analyses (Table 6) show that most maturity stages had length–mass relationships that were similar to those fitted for all krill combined. However, the fitted line for mature females was above that for all krill combined (reflecting the eggs, which visibly swell these gravid females), while that for mature males lay slightly below (Fig. 8). The slopes of the regressions for mature males and gravid females were not significantly different, although the intercepts were offset ($F_{1,53} = 37.90$, $p < 0.01$) with females 31% heavier than males of equivalent length.

Growth in mass—Growth rates are presented on a mass-specific basis for each site in Table 1, with a regional summary in Table 7. Overall, the mean growth in mass, *G*, was roughly 1% d^{-1} for the Scotia Sea for summer 2003. However, growth of individual swarms varied widely, with a maximum of 5.65% d^{-1}. The calculated growth in mass across the mainly low Chl *a* area of the Scotia Sea exceeded the mean values for the Chl *a*-rich South Georgia. This reflects both the lower temperatures and the smaller size of the krill in the south. Growth measured as mm d^{-1} declines with length, but this decline is much steeper when growth is converted to mass-specific units, due to scaling differences between these units.

Discussion

Maximum and minimum growth rates of krill in summer—Our maximum DGR values greatly exceed most previous values (Fig. 1). Are they realistic? Indeed, an equally high value from Clarke and Morris (1983) was questioned by Quetin et al. (1994). We suggest that these maxima are not artefacts for three reasons. First, when converted to units of mass, even our maximum DGR fits within a realistic energy budget, supported by measured ingestion rates (see Discussion: mass balance of krill). Second, our maxima are supported at two separate sites with >400 krill incubated. Third,

Table 6. *Euphausia superba.* Relationships between body length, *L* (mm), and dry mass, *m* (mg individual^{-1}), derived from the 2002 South Georgia Cruise. *n* = number of krill analyzed. All relationships are significant ($p < 0.001$).

Maturity stage group	Length–mass relationships	R^2 (%)	*n*
Juvenile	Log_{10} m = 4.09 $\log_{10}$ *L*–4.51	81	187
MS1–MS3	Log_{10} m = 3.67 $\log_{10}$ *L*–3.83	82	254
FS	Log_{10} m = 3.41 $\log_{10}$ *L*–3.38	72	32
FA1–FA2	No measurements	—	—
FA3–FA5	Log_{10} m = 3.74 $\log_{10}$ *L*–3.90	62	38
MA1–MA2	Log_{10} m = 3.60 $\log_{10}$ *L*–3.76	76	19
All stages combined	Log_{10} m = 3.89 $\log_{10}$ *L*–4.19	89	530

Table 7. Calculated gross increase in krill mass, *G*, using Eq. 6 and averaged by swarm. The low Chl *a* region at South Georgia is defined here by SeaWiFs-derived mean Chl *a* being <1 mg m^{-3}. *n* = number of swarms sampled.

Region	Mean daily % increase in krill mass, *G* (range)	*n*
All of Scotia Sea	1.17 (0.12–5.65)	27
South Georgia, high Chl *a* sites	1.08 (0.31–2.37)	26
South Georgia, low Chl *a* sites	0.69 (0.60–0.89)	6

they are not artefacts of our new methods because even the standard method yields maxima of 0.2–0.3 mm d^{-1} (Tarling et al. 2006). Our study included the optimum combination of conditions; small krill, cold water (<1°C), and plentiful high-quality food, so it should reveal the short term, maximum growth rates of krill.

While maximum growth rates were surprisingly high, so were the minimum values. Even in the central Scotia Sea with Chl $a < 0.2$ mg m^{-3}, krill swarms could maintain positive mean growth, despite a few individuals shrinking. Energetics models predict shrinkage at such low Chl *a* values (Hofmann and Lascara 2000; Fach et al. 2002) so our findings are unexpected. To explain how krill might survive the central Scotia Sea, Fach et al. (2002) invoked either omnivory or the location of phytoplankton patches. While these are likely, neither Chl *a* data from the ship or from SeaWiFS revealed dense phytoplankton patches here (see maximum SeaWiFS values in Table 1). Primary production was low in this region (Korb et al. 2005) and copepod abundance was low outside of blooms (Ward et al. in press). Exploiting deep Chl *a* maxima may have helped, but these were not pronounced, ubiquitous, or good predictors of krill growth. However, protozoans form background concentrations at low Chl *a* values (Fig. 4a), and ongoing work (K. Schmidt, British Antarctic Survey unpubl. data) is assessing their role in supporting krill growth.

Controls on daily growth rates—DGR comprises two distinct components: GI and IMP. How a predictor variable relates to DGR thus reflects its separate relationships to GI and to IMP (Table 8). For example, with increasing length, GI decreases and IMP lengthens, both of which lead to lower DGRs. Likewise, high temperatures reduced their GIs and lengthened their IMPs, lowering their DGRs. By contrast, food had no influence on IMP, so its effect on DGR was only through GI. Ross et al. (2000) found a similar effect of food in their experiments, but their narrower range of krill sizes and temperatures precluded analysis of how these affected growth.

Sex- and maturity stage-related differences in DGR were smaller than those related to krill length, food, or temperature, but these were nevertheless intriguing. The immature males had slightly higher GIs than immature females of similar size (Table 5) but generally longer IMPs (Tarling et al. 2006). These opposite effects appear to cancel out, so that DGRs were similar between sexes. However, DGRs for krill of a given length tended to decrease with increasing maturity stage, regardless of sex. This is likely a result of progressive diversion of available energy away from somatic growth and into reproduction.

Of the environmental variables, food had the strongest effect on growth. Our various food indices integrate over a very wide range of scales, and those at both the smallest and the largest scale could have been used to predict growth (Table 4). This reflects the strong correlation between Chl *a* measured across this spectrum of scales (Fig. 4b). So at the ocean basin scale, the great contrast between bloom and nonbloom regions overrides local patchiness. The similar growth of neighboring swarms at a site (Fig. 3) supports this explanation. Large-scale SeaWiFS food proxies are thus useful, and indeed, these provided the best predictions of krill growth (Table 4).

The importance of food quality for grazers is stressed repeatedly (e.g., Pond et al. 1993; Schmidt et al. 1998). For krill at the Antarctic Peninsula, diatoms support higher growth rates than *Phaeocystis* spp. (Ross et al. 2000), while the role of heterotrophic foods is still unclear (e.g., Schmidt et al. 2003). Despite these subtleties, our study is a reminder that also, simply, the quantity of food can be key. In this study, diatoms were dominant, with *Phaeocyctis* spp. almost absent. Protozoans (Fig. 4a) and copepods (Ward et al. in press) reached maximum abundance in these blooms; together, this whole assemblage means good-quality food (Pond et al. 1993, 2005). Blooms thus provide localized

Table 8. Summary of relationships between krill growth rate and predictor variables. Those for GI and DGR are from this article, while those with IMP are from Tarling et al. (2006).

Predictor variables	Response of components of krill growth		
	GI	IMP	DGR
Body length	Quadratic (decreasing with length)	Linear (complex, maturity-stage specific), general increase with length	Quadratic (max at 16 mm)
Food	Positive (hyperbolic)	None	Positive (hyperbolic)
Temperature	Quadratic (max at 0.6°C)	Quadratic (complex, maturity-stage specific)	Quadratic (max at 0.4°C)
Maturity stage	Decrease with maturity stage	Complex, immatures mainly affected by temperature, mature krill have IMP more sensitive to their length	Decrease with maturity stage
Sex	Slightly lower in immature females than males	Generally longer in males	Very little difference between sexes of equivalent maturity stage

pulses of primary and secondary production contrasting greatly with the surrounding water. These pulses can be mapped by SeaWiFS to provide a good, large-scale prediction of krill growth for a diatom-dominated system.

The decline in DGR at high temperatures merits appraisal, as previous models invoke the opposite response (Hofmann and Lascara 2000; Fach et al. 2002). The warm-water stations were all at South Georgia, so the first question is whether our suggested temperature effect reflects instead a distinct food or predation regime here. This is unlikely because, even within the local South Georgia area (e.g., stations of 3°C or above; Fig. 5c) we still observe a decline in growth with temperature. Another possibility is that our temperature effect is actually a seasonal effect because the date of sampling is strongly and positively related to water temperature ($R^2 = 0.73$). Thus, the decline in DGR at the later sampled, warmer water stations could reflect a seasonal reallocation of energy from somatic growth to the build-up of lipid reserves for overwintering (Hagen et al. 2001; Atkinson et al. 2002). This would invoke, however, a seasonal fattening of krill within the survey period, and our data (Fig. 7) show no evidence of this.

The evidence thus points to a real effect of temperature on growth. Artificially high incubation temperatures are certainly not the cause of a reduction in growth rates, as the warmer water experiments always had slightly cooler incubation temperatures than those of the food-rich upper mixed layer. In any case, the result holds whether using in situ or incubation temperature (model 3 versus model 5). The simplest and most plausible explanation is based on stenothermy. The 5°C temperature range of our study would be unremarkable for a boreal species, but for krill, it is almost their entire range. Antarctic benthic invertebrates suffer 50% losses of activity at 2–3°C and complete losses at 5°C (Peck et al. 2004). This reflects rapid increases in respiration cost with temperature and the onset of anaerobic metabolism (Peck et al. 2004). We therefore suggest that the slow growth rates at the northern limit of krill's range reflect the onset of thermal stress.

Implications for regional population dynamics—Over half of the Southern Ocean krill stocks are located within the southwest Atlantic sector (Atkinson et al. 2004) and the main fisheries are here. Krill population dynamics in this sector is thus a topic of intense research interest (e.g., Murphy and Reid 2001; Siegel et al. 2004). In this respect, a prime and unresolved issue is whether one or more separate stocks of krill exist across the southwest Atlantic sector (Reid et al. 2002). Clarification of this requires the separation of the dual effects of growth and mortality, which are regionally variable and poorly known, but together shape the length–frequency distributions.

The growth rates of krill at South Georgia exemplify these challenges to population dynamics. It is generally assumed that growth is maximal at South Georgia due to the warm water and plentiful food in summer (e.g., Atkinson et al. 2001; Reid et al. 2002). This was not so in our study, as growth was fastest in the more modest ice-edge blooms to the south. Three factors lead to this. First, growth is strongly length dependent. The population in the Southern Scotia Sea, both in 2003 (Fig. 2a) and in other seasons (e.g., Siegel et al. 2004), comprise the fastest growing small krill, normally rare at South Georgia (Murphy and Reid 2001). Second, temperatures at South Georgia were above the thermal optimum for krill. Third, krill do not need dense blooms for high growth rates, 1–2 μg Chl *a* L^{-1} being sufficient in our study (Fig. 6).

Thus, South Georgia may not be such an optimum environment for krill as once thought. It does have a long productive season (Atkinson et al. 2001), but summer temperatures of >3°C in the food-rich layer are nowadays common. Sea temperatures have risen by ~1°C since 1925–1939 (Whitehouse et al. 1996). So possibly South Georgia has now become thermally suboptimal for krill in summer. Measuring natural temperature responses of ectotherms at their distributional limits is valuable in the context of predicting their response to future climatic change.

Within all regions, growth rates within and outside of blooms contrast greatly. In the ice-edge blooms at sta. 26 and 36, DGRs were 10-fold those from nearby nonbloom areas (Fig. 1; Table 1). If this range of DGRs were applied to a 3-month summer growing season, a 30-mm krill would grow to over 50 mm in a bloom but only to <35 mm outside one. Within this size envelope, krill could be either in their second, third, or fourth summer, according to a von Bertalanffy-type growth curve (Rosenberg et al. 1986; Siegel 1987; Murphy and Reid 2001). The aging of krill based on size, a basic requirement in population dynamics, is thus very sensitive to the time they have spent in summer blooms. These blooms are particularly variable in the southwest Atlantic sector, over regional and seasonal to interannual scales (Constable et al. 2003). To understand krill population dynamics, however, predictions of growth must also account for variability in temperature, krill size, and maturity stage as well as food.

Energy budget and turnover of krill biomass—The energy budget of krill is still uncertain due to a series of methodological problems that hamper experiments on this species. Their maximum ingestion rate is still debated (Clarke et al. 1988; cf. Pakhomov et al. 2002), but if we know their maximum growth rates, these can bound the estimates of ingestion. Maximum growth in krill mass reached 5.65% d^{-1} (Table 7). Gross growth efficiency (i.e., growth/ingestion) of zooplankton is ~0.3 (Straile 1997) and 0.26–0.32 for euphausiids (Lasker 1960, 1966). Applying this range to a 5.65% daily growth in mass gives a maximum daily ration of 18–22%, for comparison with maxima of 13% (Perissinotto et al. 1997) and 17–28% (Clarke et al. 1988). Our findings thus add to the evidence that krill are capable of fast rates of energy throughput for an animal of their size (Quetin et al. 1994).

Within the Southern Ocean, an issue of debate is the role of advection versus local production in supporting krill predators and krill fisheries (Atkinson et al. 2001; Murphy and Reid 2001; Constable et al. 2003). These questions remain unresolved, partly due to uncertainties over growth. Our study suggests that, during the summer of 2003, the gross rate of increase in krill biomass (equivalent to *G*) was roughly 1% d^{-1} across the whole Scotia Sea–South Georgia sys-

tem (Table 7). Despite the high Chl *a* at South Georgia, our calculated growth of krill mass here is lower than that across the Scotia Sea. This again underlines the importance of krill size and temperature in calculations of krill growth, as together these can offset differences in food.

Toward the prediction of krill growth—Improved models of krill growth are needed for population dynamics and fisheries-management advice to the Committee for the Conservation of Antarctic Marine Living resources (CCAMLR). Such models (Hofmann and Lascara 2000) have already been imbedded into Southern Ocean advection models (Fach et al. 2002). However, these have needed to calculate growth from complex experimental data on feeding, respiration, and assimilation, and then to convert its units from mass to length.

Our models, by contrast, predict growth in length directly. The environmental variables, Chl *a* and temperature, are accessible with remote sensing over the appropriate time and space scales. This provides a short-cut route to predicting growth rates at the ocean basin scale, in a complimentary approach to mechanistic models. Within the boundary conditions (i.e., mainly diatom-dominated systems during summer), our models 3 and 4 provide an index of the success of krill in a variable environment. This provides a step toward assessing the response of krill to future scenarios of change.

References

ATKINSON, A., B. MEYER, D. STÜBING, W. HAGEN, K. SCHMIDT, AND U. V. BATHMANN. 2002. Feeding and energy budgets of Antarctic krill at the onset of winter—II. Juveniles and adults. Limnol. Oceanogr. **47:** 953–966.

———, V. SIEGEL, E. PAKHOMOV, AND P. ROTHERY. 2004. Long-term decline in krill stock and increase in salps within the Southern Ocean. Nature **432**: 100–103.

———, M. J. WHITEHOUSE, J. PRIDDLE, G. C. CRIPPS, P. WARD, AND M. A. BRANDON. 2001. South Georgia, Antarctica: A productive, cold water, pelagic ecosystem. Mar. Ecol. Prog. Ser. **216**: 279–308.

BUCHHOLZ, F. 1985. Moult and growth in Antarctic euphausiids, p. 339–345. *In* W. R. Siegfried, P. R. Condy, and R. M. Laws [eds.], Antarctic nutrient cycles and food webs. Springer-Verlag.

CLARKE, A. 1988. Seasonality in the Antarctic marine environment. Comp. Biochem. Physiol. **90B:** 461–473.

———, AND D. J. MORRIS. 1983. Towards an energy budget for krill: The physiology and biochemistry of *Euphausia superba* Dana. Polar Biol. **2:** 69–86.

———, L. B. QUETIN, AND R. M. ROSS. 1988. Laboratory and field estimates of the rate of faecal pellet production by Antarctic krill, *Euphausia superba.* Mar. Biol. **98**: 557–563.

CONSTABLE, A. J., S. NICOL, AND P. G. STRUTTON. 2003. Southern Ocean productivity in relation to spatial and temporal variation in the physical environment. J. Geophys. Res. **108.** [doi: 101129/2001JC001270]

DALY, K. L. 1998. Physioecology of juvenile Antarctic krill (*Euphausia superba*) during spring in ice-covered seas. Ant. Res. Ser. **73:** 183–198.

DIGGLE, P., K.-Y. LIANG, AND S. L. ZEGER. 1994. Analysis of longitudinal data. Clarendon Press.

FACH, B. A., E. E. HOFMANN, AND E. J. MURPHY. 2002. Modeling studies of Antarctic krill *Euphausia superba* survival during transport across the Scotia Sea. Mar. Ecol. Prog. Ser. **231:** 187–203.

HAGEN, W., G. KATTNER, A. TERBRÜGGEN, AND E. S. VAN VLEET. 2001. Lipid metabolism of Antarctic krill *Euphausia superba* and its ecological implications. Mar. Biol. **139:** 95–104.

HOFMANN, E. E., AND C. M. LASCARA. 2000. Modeling the growth dynamics of Antarctic krill *Euphausia superba.* Mar. Ecol. Prog. Ser. **194:** 219–231.

IKEDA, T. 1985. Life history of Antarctic krill *Euphausia superba*: A new look from an experimental approach. Bull. Mar. Sci. **37:** 599–608.

KANDA, K., K. TAKAGI, AND Y. SEKI. 1982. Movement of the larger swarms of Antarctic krill *Euphausia superba* off Enderby Land during 1976–77 season. J. Tokyo Univ. Fish. **68:** 24–42.

KORB, R. E., M. J. WHITEHOUSE, S. E. THORPE, AND M. GORDON. 2005. Primary production across the Scotia Sea in relation to the physico-chemical environment. J. Mar. Systems **57:** 231–249.

LASKER, R. 1960. Utilization of organic carbon by a marine crustacean: Analysis with carbon-14. Science **131:** 1098–1100.

———. 1966. Feeding, growth, respiration and carbon utilization of a euphausiid crustacean. J. Fish. Res. Bd. Can. **23:** 1291–1317.

MACKINTOSH, N. A. 1972. Life cycle of Antarctic krill in relation to ice and water conditions. Discovery Rep. **36:** 1–94.

MCCLATCHIE, S. 1988. Food-limited growth of *Euphausia superba* in Admiralty Bay, South Shetland Islands, Antarctica. Continental Shelf Res. **8:** 329–345.

MEREDITH, M. M., AND J. C. KING. 2005. Rapid climate change in the ocean west of the Antarctic Peninsula during the second half of the 20th century. Geophys. Res. Lett. **32.** [doi: 1029/2005GL024042]

MORRIS, D. J., AND A. KECK. 1984. The time course of the moult cycle and growth of *Euphausia superba* in the laboratory: A preliminary study. Meeresforchung **30:** 94–100.

MURPHY, E. J., AND K. REID. 2001. Modelling Southern Ocean krill population dynamics: Biological processes generating fluctuations in the South Georgia ecosystem. Mar. Ecol. Prog. Ser. **217:** 175–189.

NICOL, S. 2000. Understanding krill growth and aging: The contribution of experimental studies. Can. J. Fish. Aquat. Sci. **57:** 168–177.

———, M. STOLP, T. COCHRAN, P. GEIJSEL, AND J. MARSHALL. 1992. Growth and shrinkage of Antarctic krill *Euphausia superba* from the Indian Ocean Sector of the Southern Ocean during summer. Mar. Ecol. Prog. Ser. **89:** 175–181.

ORSI, A. H., T. WHITWORTH III, AND W. D. J. NOWLIN. 1995. On the meridional extent and fronts of the Antarctic Circumpolar Current. Deep-Sea Res. I **42:** 641–673.

PAKHOMOV, E. A. 2000. Demography and life cycle of Antarctic krill, *Euphausia superba,* in the Indian sector of the Southern Ocean: Long-term comparison between coastal and upwelling regions. Can. J. Fish Aquat. Sci. **57:** 68–90.

———, P. W. FRONEMAN, AND R. PERISSINOTTO. 2002. Salp/krill interactions in the Southern Ocean: Spatial segregation and implications for the carbon flux. Deep-Sea Res. II **49:** 1881–1907.

PARKINSON, C. L. 2002. Trends in the length of the Southern Ocean sea-ice season, 1979–99. Ann. Glaciol. **34:** 435–440.

PARSONS, T. R., Y. MAITA, AND C. M. LALLI. 1984. A manual of chemical and biological methods of seawater analysis. Pergamon.

PECK, L. S., K. E. WEBB, AND D. M. BAILEY. 2004. Extreme sensitivity of biological function to temperature in Antarctic marine species. Funct. Ecol. **18:** 625–630.

PERISSINOTTO, R., E. A. PAKHOMOV, C. D. MCQUAID, AND P. W.

FRONEMAN. 1997. In situ grazing rates and daily ration of Antarctic krill *Euphausia superba* feeding on phytoplankton at the Antarctic Polar Front and the Marginal Ice Zone. Mar. Ecol. Prog. Ser. **160:** 77–91.

POND, D. W., A. ATKINSON, R. S. SHREEVE, G. TARLING, AND P. WARD. 2005. Diatom fatty acid biomarkers indicate recent growth rates in Antarctic krill. Limnol. Oceanogr. **50:** 732–736.

———, J. PRIDDLE, J. R. SARGENT, AND J. L. WATKINS. 1993. Lipid composition of Antarctic microplankton in relation to the nutrition of krill, p. 133–139. *In* R. B. Heywood [ed.], University Research in Antarctica. British Antarctic Survey.

QUETIN, L. B., AND R. M. ROSS. 2001. Environmental variability and its impact on the reproductive cycle of Antarctic krill. Am. Zool. **41:** 74–89.

———, ———, AND A. CLARKE. 1994. Krill energetics: Seasonal and environmental aspects of the physiology of *Euphausia superba,* p. 165–184. *In* S. Z. El-Sayed [ed.], Southern Ocean ecology: The BIOMASS perspective. Cambridge University Press.

REID, K. 2001. Growth of Antarctic krill *Euphausia superba* at South Georgia. Mar. Biol. **138:** 57–62.

———, E. J. MURPHY, V. LOEB, AND R. P. HEWITT. 2002. Krill population dynamics in the Scotia Sea: Variability in growth and mortality within a single population. J. Mar. Systems **36:** 1–10.

ROSENBERG, A. A., J. R. BEDDINGTON, AND M. BASSON. 1986. Growth and longevity of krill during the first decade of pelagic whaling. Nature **324:** 152–153.

ROSS, R. M., L. B. QUETIN, K. S. BAKER, M. VERNET, AND R. C. SMITH. 2000. Growth limitation in young *Euphausia superba* under field conditions. Limnol. Oceanogr. **45:** 31–43.

SCHMIDT, K., A. ATKINSON, D. STÜBING, J. W. MCCLELLAND, J. P. MONTOYA, AND M. VOSS. 2003. Trophic relationships among Southern Ocean copepods and krill: Some uses and limitations of a stable isotope approach. Limnol. Oceanogr. **48:** 277–289.

———, P. KÄHLER, AND B. VON BODUNGEN. 1998. Copepod egg production rates in the Pomeranian Bay (southern Baltic Sea) as a function of phytoplankton abundance and taxonomic composition. Mar. Ecol. Prog. Ser. **174:** 183–195.

———, J. W. MCCLELLAND, E. MENTE, J. P. MONTOYA, A. ATKINSON, AND M. VOSS. 2004. Trophic-level interpretations based on δ^{15}N values: Implications of tissue-specific fractionation and amino acid composition. Mar. Ecol. Prog. Ser. **266:** 43–58.

SHREEVE, R. S., G. A. TARLING, A. ATKINSON, P. WARD, C. GOSS, AND J. L. WATKINS. 2005. Relative production of *Calanoides acutus* (Copepoda: Calanoida) and *Euphausia superba* (Antarctic krill) at South Georgia and its implications at wider scales. Mar. Ecol. Prog. Ser. **298:** 229–239.

SIEGEL, V. 1987. Age and growth of Antarctic Euphausiacea (Crustacea) under natural conditions. Mar. Biol. **96:** 483–495.

———, S. KAWAGUCHI, P. WARD, F. LITVINOV, V. SUSHIN, V. LOEB, AND J. L. WATKINS. 2004. Krill demography and large-scale distribution in the southwest Atlantic during January/February 2000. Deep-Sea Res. II **51:** 1253–1273.

STRAILE, D. 1997. Gross growth efficiencies of protozoan and metazoan zooplankton and their dependence on food concentration, predator–prey weight ratio, and taxonomic group. Limnol. Oceanogr. **42:** 1375–1385.

TARLING, G. A., R. S. SHREEVE, A. G. HIRST, A. ATKINSON, D. W. POND, E. J. MURPHY, AND J. L. WATKINS. 2006. Natural growth rates in Antarctic krill (*Euphausia superba*): I. Improving methodology and predicting intermoult period. Limnol. and Oceanogr. **51:** 959–972.

THORPE, S. E., K. J. HEYWOOD, M. A. BRANDON, AND D. P. STEVENS. 2002. Variability of the southern Antarctic Circumpolar Current front north of South Georgia. J. Marine Systems **37:** 87–105.

UTERMÖHL, H. 1958. Zur Vervollkommnung der quantitativen Phytoplankton-Methodik. Verh. Int. Limnol. **9:** 1–38.

VAUGHAN, D. G., AND OTHERS. 2003. Recent rapid regional climate warming on the Antarctic Peninsula. Climatic Change **60:** 243–274.

WARD, P., AND OTHERS. A. In press. Plankton community structure and variability in the Scotia Sea: austral summer 2003. Mar Ecol. Prog. Ser.

———, AND OTHERS. 2005. Phyto- and zooplankton community structure and production around South Georgia (Southern Ocean) during summer 2001/02. Deep-Sea Res. I. **52:** 421–441.

WHITEHOUSE, M. J., J. PRIDDLE, AND C. SYMON. 1996. Seasonal and annual change in seawater temperature, salinity, nutrient and chlorophyll *a* distributions around South Georgia, South Atlantic. Deep-Sea Res. **43:** 425–443.

Received: 14 February 2005
Accepted: 7 September 2005
Amended: 27 September 2005